Hydration-mediated stiffening of collective membrane dynamics by cholesterol

Journal:	*Physical Chemistry Chemical Physics*
Manuscript ID	CP-ART-03-2019-001431.R1
Article Type:	Paper
Date Submitted by the Author:	13-Apr-2019

Complete List of Authors:	Päslack, Christopher; Ruhr-University Bochum, Theoretical Chemistry Smith, Jeremy; Oak Ridge National Laboratory, UT/ORNL Center for Molecular Biophysics Heyden, Matthias; Arizona State University, School of Molecular Sciences Schäfer, Lars; Ruhr-University Bochum, Theoretical Chemistry

Journal Name

ARTICLE TYPE

Cite this: DOI: 00.0000/xxxxxxxxxx

Hydration-mediated stiffening of collective membrane dynamics by cholesterol†

Christopher Päslack*[a], Jeremy C. Smith[b], Matthias Heyden[c] and Lars V. Schäfer*[a]

Received Date
Accepted Date

DOI: 00.0000/xxxxxxxxxx

The collective behaviour of individual lipid molecules determines the properties of phospholipid membranes. However, the collective molecular motions often remain challenging to characterise at the desired spatial and temporal resolution. Here we study collective vibrational motion on picosecond time scales in dioleoylphosphatidylcholine lipid bilayers with varying cholesterol content using all-atom molecular dynamics simulations. Cholesterol is found to not only laterally compact the lipid bilayer, but also to change the velocity of longitudinal density fluctuations propagating in the plane of the membrane. Cholesterol-induced reduction of the area per lipid alters the collective dynamics of the lipid headgroups, but not of the lipid tails. The introduction of cholesterol reduces the number of water molecules interacting with the lipid headgroups, leading to a decrease in the velocity of the laterally-propagating sound mode. Thus, the stiffening effect of cholesterol is found to be indirect: decreasing the area per lipid weakens the interactions between the lipid headgroups and water. The collective modes characterised in this work can enable the membrane to dissipate excess energy and thus maintain its structural integrity, e.g., under mechanical stress.

1 Introduction

Biological membranes are key constituents of all cells, defining the cell boundaries, enclosing organelles, and regulating the transport of molecules into and out of the cell. Cell membranes are usually composed of a complex mixture of different lipid species, with phospholipids being the most abundant lipid type in both prokaryotes and eukaryotes. At physiological conditions, many lipid bilayers are in a liquid-crystalline phase with disordered alkyl chains, giving rise to membrane fluidity. Since the 1970s, the original fluid mosaic model[1] has been refined leading to more complex models, which include that lateral heterogeneities in the membrane can influence their structure and dynamics[2–4]. The fluidity of lipid bilayers is regulated by their composition, with sterols such as cholesterol playing a major role in higher vertebrate plasma membranes[5–8]. Due to its planar tetracyclic ring, cholesterol compacts the membrane by intercalating between the lipid tails. This increases the ordering of the alkyl chains and leads to a reduced area per lipid (APL) and an increased thickness of the lipid bilayer[9,10].

The physical properties of phospholipid membranes are influenced by the collective dynamics of lipid molecules[11–13]. Membranes exhibit motions on a wide range of time and length scales, with peristaltic and undulatory motions on the ns time scale[14] as prominent examples. Moreover, inelastic x-ray scattering[15], inelastic neutron scattering[13,16], and molecular dynamics (MD) simulations[17] have demonstrated that lipid bilayers exhibit collective short-wavelength dynamics showing dispersion, *i.e.*, correlated density fluctuations on the sub-ps time scale. Such dispersive modes arise from in-plane (lateral) motions of the lipids. Their frequency and damping depends on the lipid phase. Furthermore, MD simulations of dipalmitoylphosphatidylcholine (DPPC) bilayers showed that external mechanical stress propagates laterally through lipid bilayers at a velocity around 1400 m/s, very similar to the collective acoustic modes observed experimentally[18].

The short-range order and short-wavelength dynamics of a pure dimyristoylphosphatidylcholine (DMPC) bilayer were studied by Hub *et al.*[19]. The interchain distance can be computed from the interchain correlation peak of the static structure factor. Moreover, the position of the interchain correlation peak does not depend on the area per lipid (APL), while the correlation length decreases linearly with the APL[19].

[a] *Theoretical Chemistry, Faculty of Chemistry and Biochemistry, Ruhr University Bochum, D-44780 Bochum, Germany. E-mail: christopher.paeslack@ruhr-uni-bochum.de , lars.schaefer@ruhr-uni-bochum.de; Tel: +49-234-3221582*
[b] *Center for Molecular Biophysics, Oak Ridge National Laboratory, Oak Ridge, Tennessee 37831, USA and Department of Biochemistry and Cellular and Molecular Biology, University of Tennessee, Knoxville, Tennessee 37996, USA*
[c] *School of Molecular Sciences, Arizona State University, Tempe, AZ 85287-1604, USA*
† Electronic Supplementary Information (ESI) available. See DOI: 10.1039/b000000x/

An open question is whether and if so, how exactly cholesterol affects the "communication" between lipids in terms of collective short-wavelength dynamics. Although there are indications that collective lipid dynamics may play an important role for the regulation of membrane protein function and membrane permeability[20,21], the effects of sterols on these modes remain largely unexamined so far.

This work aimed to elucidate in atomic detail the interplay between cholesterol-induced changes of membrane properties and collective lipid motions. To this end, we carried out all-atom MD simulations of dioleoylphosphatidylcholine (DOPC)/cholesterol bilayers as model systems because these bilayers are in the liquid-crystalline (L_α) phase under the investigated conditions. The results reveal how cholesterol modulates the propagation velocity of the dispersive acoustic modes that originate from correlated velocity fluctuations of lipid atoms. Cholesterol-induced lateral compactification of the bilayer decreases the number of water molecules per lipid headgroup (*i.e.,* in the first hydration shell), thus reducing the velocity of the hydration-dependent lateral sound modes of the lipid headgroups. Hence, hydration provides a microscopic link between the short-wavelength dynamics and macroscopic properties such as area per lipid.

2 Methods

2.1 Molecular dynamics simulations

We used pre-equilibrated DOPC membranes with cholesterol contents of 0–50 mol-% from Jämbeck *et al.* [22,23]. All-atom molecular dynamics (MD) simulations were carried out for bilayers composed of 512 lipids in total (256 in each leaflet). We further equilibrated the simulation systems for 25 ns in the isothermal-isobaric (NPT) ensemble at 300 K and 1 bar; the bilayers are in the liquid-disordered phase under these conditions. Figure 1 shows the simulation systems and molecular structures of DOPC and cholesterol; see also Figures S1 and S2 in the Electronic Supplementary Information (ESI†). For each cholesterol concentration, ten starting structures were extracted from the last 10 ns of the NPT equilibrations to initiate the subsequent production simulations in the microcanonical (NVE) ensemble. The NVE simulations were carried out for 1 ns each, with positions and velocities saved to disk every 20 fs to sample the fast vibrational motions. Results were obtained by averaging over the 10 NVE simulations for each cholesterol concentration. Simulation details can be found in the ESI†.

2.2 Analysis of collective dynamics

We analysed the collective dynamics of the lipid bilayers via lateral correlated velocity fluctuations, *i.e.*, spectral densities computed from time cross-correlation functions of mass-weighted atomic velocities. Using the time-correlation formalism a generalised vibrational density of states (VDOS) is defined,

$$I(\omega,d) = \int e^{-i\omega t} \left\langle \tilde{\mathrm{v}}_i(\tau,\mathrm{r}_i) \cdot \tilde{\mathrm{v}}_j(\tau+t,\mathrm{r}_j) \right\rangle_\tau dt \qquad (1)$$

with $d = |\mathrm{r}_i - \mathrm{r}_j|$ and $\tilde{\mathrm{v}} = \sqrt{m}\mathrm{v}$, giving an expression proportional to the thermal energy for auto-correlations ($i = j$). The brackets

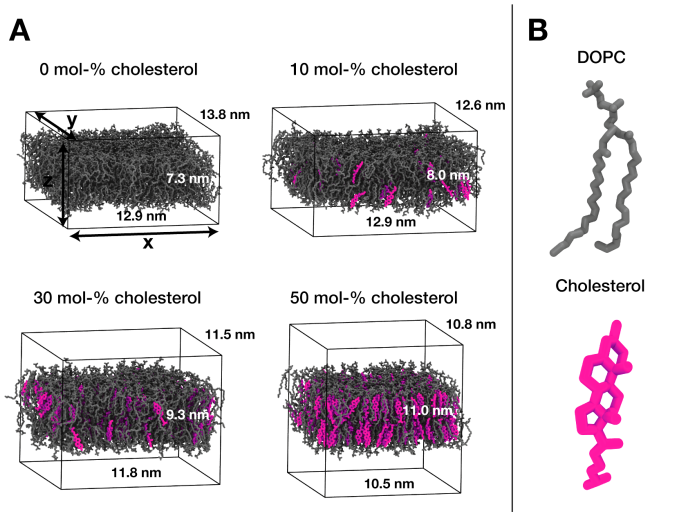

Fig. 1 A) Lipid bilayers with 0–50 mol-% cholesterol content, each containing 512 lipids in total. DOPC and cholesterol molecules are shown in gray and magenta, respectively. Water molecules are not shown for clarity. The average lengths of the box vectors are indicated. B) Structures of DOPC and cholesterol.

$\langle \ldots \rangle_\tau$ denote ensemble averages. Equation 1 describes correlated velocity fluctuations of distinct atoms $i \neq j$ at their respective positions r_i and r_j (see Ref. 24). Overall translation of the bilayer was removed prior to analysis. The analysis was restricted to non-hydrogen atoms, because heavy atoms dominate the vibrational density of states at frequencies below 400 cm^{-1}. The frequencies of the analysed collective vibrations correspond to time scales of ca. 0.5–1.5 ps. We focused our analysis on the longitudinal components of the velocity vectors in the x,y-plane (perpendicular to the membrane normal), so that the collective dynamics are related to laterally propagating acoustic modes[24,25]. The ensemble-averaged cross-correlation functions are time-symmetric at equilibrium, and thus one can distinguish positive and negative intensities in the spectral densities, corresponding to parallel and antiparallel vibrations, respectively, of the correlated velocity vectors at a given frequency. We performed the analysis of velocity cross-correlations separately for lipid headgroup, lipid alkyl tail and center-of-mass (COM) velocities (see Figure S3, ESI†, for atom selections).

In analogy to coherent scattering data, we visualise the resulting spectra as function of inverse distance $k = 2\pi/d$. The k-resolved spectra $I(\omega,k)$ describe correlated density fluctuations and hence are related to the dynamic structure factor $I(\omega,k) = (\omega^2/k^2) \cdot S_{coh}(\omega,k)$ [26]. By applying the dispersion relation $v_l = d\omega/dk$ to the linear regime of the negative-intensity peak trace, we identify longitudinal collective modes propagating through the lipid bilayer in the plane of the membrane.

Our analysis focuses on lipid–lipid distances d in the hydrodynamic limit, because at $k < 1.2$ Å^{-1} ($d \gtrsim 5$ Å) the wavelengths are larger than the typical interchain distances, *i.e.*, near the interchain correlation peak of the static structure factor. In the hydrodynamic limit, the mode frequency ω increases linearly with wavenumber k and one can use the dispersion relation to determine the propagation velocity v_l of such acoustic modes. For

higher k-values ($k \approx 1.3$ Å^{-1}), the dispersion relation exhibits the so-called "dispersion gap" of the propagating sound mode as the wavelength approaches the interchain distance. Because we considered exclusively the region below the dispersion gap, it was required to simulate sufficiently large membranes containing 256 lipids per leaflet in order to study the long-range/low-k collective dynamics of many lipids in a periodic simulation cell.

Finally, we also analysed the collective dynamics between lipid headgroups and hydration water molecules. To that end, we employed localised density kernels $\rho_{\tilde{v}}(r) \approx \sum_i \tilde{v}_i((2\pi\sigma^2)^{3/2})^{-1/2}\exp[-(|r_i - r|^2/2\sigma^2)]$ of mass-weighted velocities $\tilde{v} = m_i v$ for water oxygen atoms, to account for the fast displacements of the water molecules[24]. Water molecules were considered up to distances of 10 Å from the membrane surface. The dispersion relations were analysed for both the ordinary sound mode (0.60–0.90 Å^{-1}) and the fast sound mode (1.00–1.60 Å^{-1}).

3 Results and discussion

3.1 Cholesterol modulates collective lipid motions

For each of the simulated systems, the pair-wise cross-correlation spectra $I(\omega,d)$ of each lipid atom (or center-of-mass) with atoms of surrounding lipids at distances of 6 Å $\leq d \leq$ 30 Å (in steps of 3 Å) were computed according to Eq. 1. The average spectrum for each distance was then obtained by averaging over all lipids. Figure 2A) shows the cross-correlation spectra for the pure DOPC bilayer calculated for the lipid headgroups in the left panel; the distance d is illustrated in the right panel. We observe dispersion of the negative-intensity modes, *i.e.*, a decrease of vibration frequency with increasing distance d. Interestingly, atoms are still weakly correlated with each other at large distances up to $d = 20$–30 Å, where the correlation intensity has however dropped strongly (by ca. 90 %) compared to interchain contact at $d = 6$ Å. The interchain contact region can be identified from the lateral radial distribution functions $g(r)$ of the lipids (Figure S4, ESI†).

As mentioned above, we analysed the propagation velocity v_l of collective lipid–lipid modes. Analysing the spectra as a function of inverse distance k and following the trace of the negative-intensity peak, the propagation velocity of the corresponding collective vibrational mode can be obtained from the dispersion relation. The linear fit to the dispersion relation was applied within the range $0.2 \leq k \leq 0.6$ Å^{-1}, which corresponds roughly to distances of 10–30 Å. Figure 3 shows the cross-correlation spectra of lipid headgroup atoms as a function of k for systems with varying cholesterol content. The mode velocity decreases with increasing cholesterol concentration, from 1562 ± 43 m/s for the pure DOPC bilayer to 1224 ± 21 m/s for 50 mol-% cholesterol. Convergence of the spectra was tested by analyzing only 500 ps (instead of 1 ns) of each of the 10 NVE trajectories for 0 mol-% cholesterol, yielding a similar mode velocity of 1580 ± 27 m/s for the headgroups (Figure S5, ESI†).

Rheinstädter *et al.* have characterised the different regimes (time scales and wave vectors) of collective excitations in lipid bilayers using neutron scattering techniques[16]. According to their categorization, the collective vibrations that we describe in this work (on a time scale of 0.5–1.5 ps and in a k-range of 0.2–1.0 Å^{-1}) can indeed be characterised as "propagating modes", in contrast to relaxing (overdamped) or localised oscillating modes.

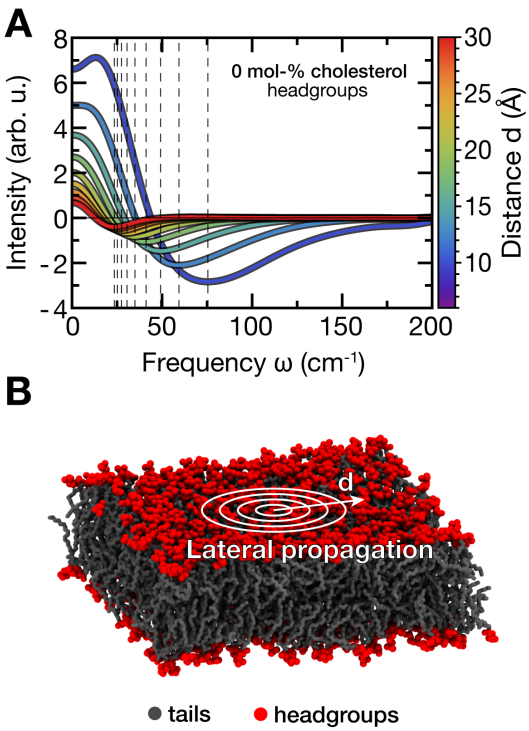

Fig. 2 A) Lipid–lipid cross-correlation spectra $I(\omega,d)$ of mass-weighted atomic velocities computed at different lipid atom–lipid atom distances d. Shown are the results for headgroups of the pure DOPC bilayer. Gray dashed lines highlight the positions of the negative-intensity peaks for each distance. All spectra were smoothed using Gaussian window functions of width 10 cm^{-1}. B) Top view of a simulation box of a pure DOPC bilayer with an illustration of the definition of the lateral atom–atom distances d (white circles and arrow). Velocities were projected on the connecting vectors to obtain the longitudinal components.

To investigate whether and how the propagation velocity v_l of the collective modes is linked to the lateral structure of the lipid bilayers, we analysed v_l as a function of the area per lipid. Figure 4A shows a strong linear correlation between these two quantities for the lipid headgroups (red data points), suggesting that lateral density is a key modulator of the collective dynamics on the ps time scale. However, in contrast to the headgroups, the propagation velocities for the lipid tails and COMs are invariant with respect to the lateral packing (Figure 4A, orange and green data points). To rule out a box-size dependence of the observed effects, control simulations of a smaller bilayer with 178 DOPC lipids per leaflet were performed, yielding a velocity of 1555 ± 50 m/s, in close agreement with the value obtained for the larger systems. The mode velocity was further confirmed by control simulations of a pure DOPC bilayer in the presence of 150 mM NaCl, which yielded 1575 ± 28 m/s (Figure S5, ESI†).

3.2 Hydration determines the collective dynamics of lipid headgroups

To answer the question why the collective dynamics of only the lipid headgroups, but not the tails, are affected by the lateral

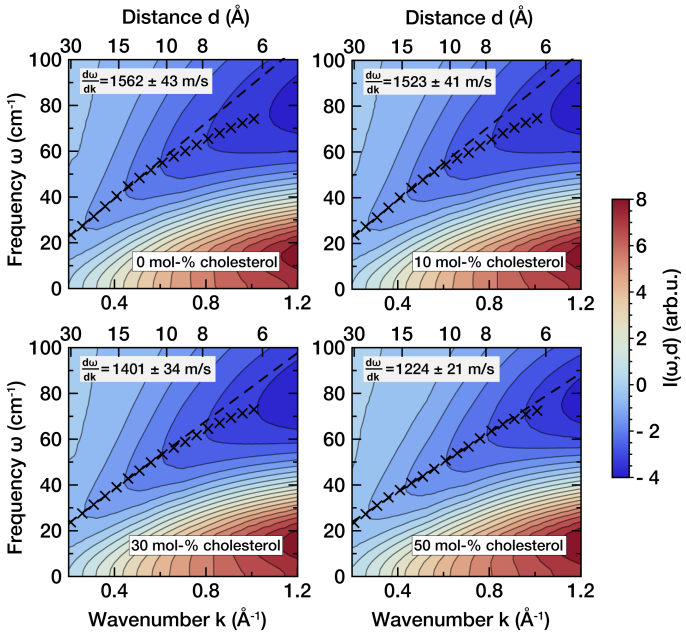

Fig. 3 Lipid–lipid cross-correlation spectra $I(\omega,d)$ of mass-weighted atomic velocities (Eq. 1). The spectra show correlated vibrations of non-hydrogen lipid atoms as a function of reciprocal distance $k = 2\pi/d$. For each distance d the corresponding spectrum is shown. Black points trace the peak intensity of the negative-intensity modes. Dashed lines indicate linear dispersion curves of the negative-intensity peaks fitted up to $k = 0.6$ Å^{-1}.

packing density, the wave velocities were correlated with the average number of hydration water molecules per lipid, N_{hydwat}. This number was obtained by counting the average number of water molecules within 5 Å of a DOPC phosphorus atom or a cholesterol oxygen atom. Figure 4B shows that the wave velocities increase linearly with N_{hydwat} for the headgroups, suggesting that changes in the couplings between the headgroup atoms and water molecules in the first hydration shells play a role for the collective dynamics of the lipid headgroups. To test that hypothesis, we computed the lipid–water cross-correlation spectra and analysed both the ordinary sound mode and the fast sound mode[27]. For both modes, the correlated density fluctuations propagate slower for higher cholesterol concentrations, *i.e.*, less hydration water molecules per lipid headgroup (Figure S6, ESI†).

Interestingly, for the pure DOPC bilayer (0 mol-% cholesterol) the velocity of the lipid–water ordinary sound mode v_{low} is very close to the ordinary sound velocity in bulk water, around 1500 m/s. Changes in the ordinary sound velocity v_{low} of propagating lipid–water correlations follow the same trend with increasing cholesterol concentrations as collective mode velocities v_l between lipid headgroups in the membrane plane. This supports the notion that hydration plays an important role for the lipid headgroup collective dynamics.

To corroborate this finding, we performed additional simulations of the pure DOPC bilayer in which we doubled the masses of the water atoms. For the headgroups, the mode velocity increases to $v_l = 1843 \pm 17$ m/s, which is considerably higher than in regular water. As expected, the mode velocities of tails and COMs

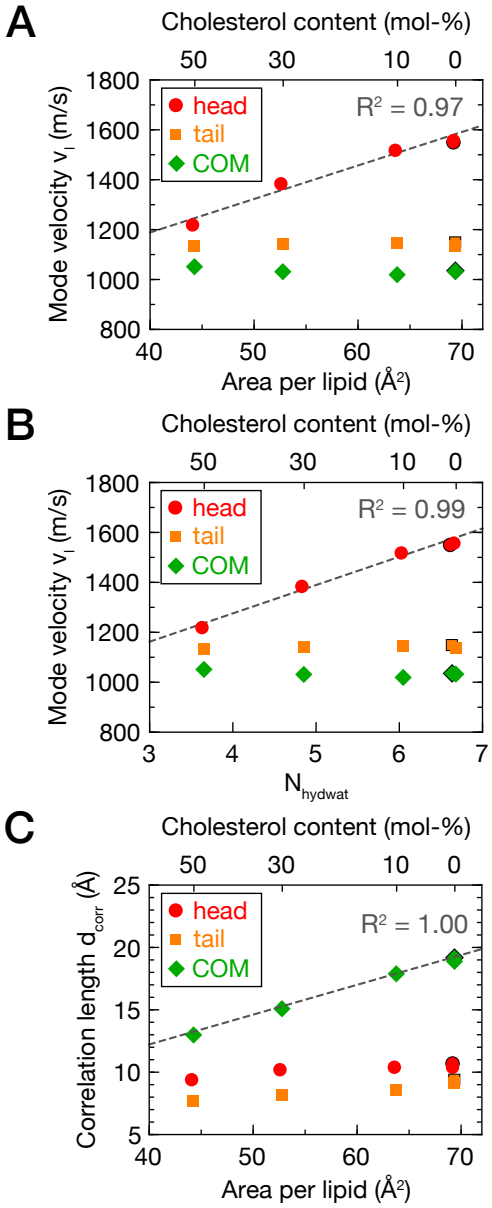

Fig. 4 A) Correlation plot of the mode velocities v_l and the average area per lipid for different cholesterol concentrations. B) Correlation of the mode velocities v_l and the number of hydration waters per lipid N_{hydwat} for 0–50 mol-% cholesterol. C) Correlation length d_{corr} of the decay of cross-correlation intensity as a function of area per lipid. Shown are the results for lipid headgroups (red circles), alkyl tails (orange diamonds) and lipid center-of-mass (green triangles). For the pure DOPC bilayer (0% cholesterol), the data points for the systems with 256 and 178 lipids per leaflet are shown (the latter are indicated by black margins).

remain unchanged within the statistical errors (1135 ± 22 m/s and 1047 ± 14 m/s, respectively).

In line with our findings, Hub *et al.* indicated differences in the collective dynamics of lipid headgroups and alkyl tails originating from the presence of water near the headgroups[19]. They compared the actual lateral lipid distributions to predictions from a simple liquid theory based on packing of beads on a two-dimensional hexagonal lattice, for which the distances between adjacent lipid headgroups and tails are $(2 \cdot APL/\sqrt{3})^{1/2}$ and

$(APL/\sqrt{3})^{1/2}$, respectively. For a pure DMPC bilayer the value of ~ 8.5 Å for the lipid headgroups derived from this simple geometric model compares very well to the actual headgroup peak at ~ 8.7 Å in the lateral radial distribution function (RDF) [19]. However, the simple model fails to correctly describe the packing of the lipid tails. Our results are in agreement with this observation, as can be seen from the RDFs of lipid tails and headgroups (Figure S4, ESI†). The simple packing model yields a nearest-neighbor distance of ca. 9.0 Å ($k \approx 0.7$ Å^{-1}) for DOPC headgroups at 300 K, which agrees with the peak in the headgroup RDF. For the lipid tails, however, the simple model predicts a value of ca. 6.3 Å ($k \approx 1.0$ Å^{-1}), which is higher than the actual value of around 5.0 Å ($k \approx 1.3$ Å^{-1}) in the RDF. Our findings hence provide insights into why the dynamics of the lipid chains cannot be described satisfactorily by the simple hexagonal lattice model.

Next, we analysed the correlation length d_{corr} of the collective lipid–lipid modes, which is the distance at which the intensity of the negative peak has dropped to $1/e$ of its value at the interchain contact distance of $d = 6$ Å. We obtained d_{corr} by fitting an exponential function to the peak intensities (see Figure S7 in the ESI† for the fit curves obtained for lipid headgroups, alkyl tails and COMs). Figure 4C shows the correlation length as a function of area per lipid. We find that the correlation length depends on the area per lipid, and up to values close to the reference area per lipid (69.4 Å^2 for the pure DOPC bilayer) the correlation length increases linearly. The linear increase is more pronounced for the lipids center-of-mass than for the headgroups or lipid tails.

3.3 Dissipation of thermal energy through the collective modes

We complemented the characterization of correlated velocity fluctuations in lipid bilayers by a time-domain analysis. For membrane–water collective vibrations the thermal energy exchanged along the connecting vector between correlated atoms (relative to the thermal fluctuations at equilibrium) can be interpreted as dynamic information. The top panel of Figure 5 shows the time cross-correlation functions (TCCFs) of velocities evaluated for the lipid headgroups of the bilayers with 0 mol-% and 50 mol-% cholesterol. The thermal energy exchange occurs on a time scale of a few picoseconds. Reassuringly, we find for the pure DOPC membrane that the energy transport over 30 Å distance takes about 2 ps, which is in accordance with the mode velocity of about 1500 m/s obtained from the dispersion relation of the longitudinal current spectra. For 50 mol-% cholesterol the transport takes about 25% longer, which is also in expected agreement with the slightly slower mode velocity of about 1200 m/s.

Finally, we analysed the distance dependence of the thermal energy dissipation via the collective modes. Since the time cross-correlation function is a generalization of the velocity autocorrelation function C_{vv}, which for zero correlation time yields the average thermal energy per degree of freedom, one can interpret the negative-intensity correlation in terms of the thermal energy of the collective mode. Figure 5B, left panel shows the decay of the relative thermal energy with lipid–lipid distance, *i.e.*,

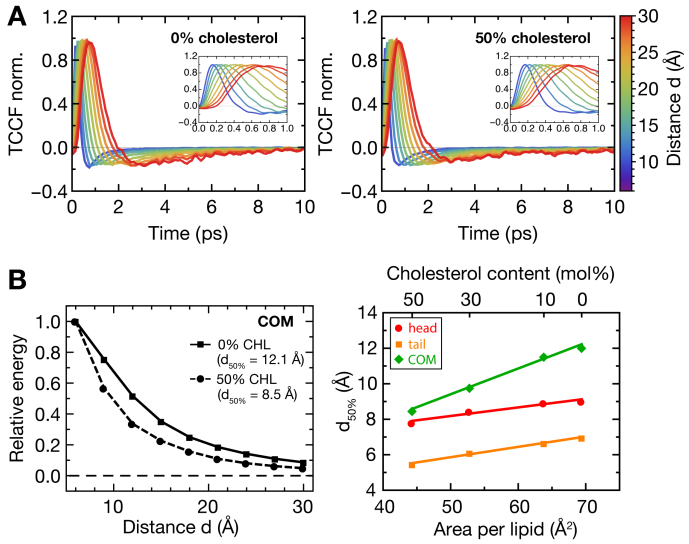

Fig. 5 A) Time cross-correlation functions of correlated velocity fluctuations of the lipids for 0 mol-% cholesterol (left) and 50 mol-% cholesterol (right). B) Decay of the relative thermal energy of the correlated vibrations with lipid–lipid distance for the lipid COMs (left) and the dissipation distances $d_{50\%}$ of the relative thermal energy as a function of area per lipid, obtained from exponential fits to the decay curves (right).

the negative-intensity correlation normalised by the value at contact distance ($d = 6$ Å). At contact distance, the thermal energy of the correlated atoms in this single degree of freedom amounts to about 1% of their total thermal energy (Figure S8, ESI†). At roughly 8–12 Å distance, the thermal energy in the propagating mode has dropped to 50% of the value at 6 Å. The decays depend on the cholesterol content and are thus determined by the area per lipid. Again, the most pronounced changes are found for lipid COMs, as shown on the right of Figure 5B. Interestingly, the variation of the dissipation distance $d_{50\%}$ with cholesterol content (or area per lipid) is smallest for the lipid headgroups. A reason may be that, compared to the lipid tails, the lipid headgroups additionally dissipate energy into the hydration water.

4 Conclusions

We studied collective dynamics of lipid bilayers in the liquid-crystalline phase. More specifically, we investigated the lateral correlated velocity fluctuations of the lipids with varying cholesterol content. The collective motions occur on ps- to sub-ps time scales (< 100 cm^{-1}) and were analysed in terms of longitudinal current spectra of velocity fluctuations. The dispersion relation was used to obtain propagation velocities of the lateral acoustic modes.

Lateral propagation of the collective modes occurs in the regime of ordinary sound in bulk water. The propagation velocities are different for the headgroups, tails, and centers-of-mass of the lipids. Moreover, the collective vibrations of the headgroups are affected by the cholesterol concentrations. The linear decrease of the mode velocity v_l with increasing cholesterol concentration can be attributed to the decreasing area per lipid. Lateral compactification of the membrane leads to a decrease of

the number of hydration water molecules in the first solvation shell of the lipid headgroups, N_{hydwat}. The structure and dynamics of water at the interface of phospholipid bilayers have been intensely researched, by both experimental techniques and molecular simulations[28–34]. Interestingly, we found that the alteration of the lateral mode propagation correlates with a change in N_{hydwat}, suggesting a coupling of the collective dynamics of the lipid headgroups to their hydration shells. This is in line with previous reports of correlated motions between phospholipid headgroups and individual water molecules (as opposed to the collective dynamics analysed here), which persist on time scales of 20–100 ps[31]. Our analyses of the collective lipid–water vibrations provide further support for this idea. Both the ordinary and the fast sound mode depend on the lateral packing of the lipids, *i.e.*, the mode propagation becomes slower for denser packing. We conclude that for areas per lipid close to the reference value of a pure DOPC bilayer, there are enough hydration water molecules present to dictate the collective dynamics of the lipid headgroups. When the area per lipid decreases, the amount of water in the lipid headgroup region is reduced and the collective dynamics of the headgroups become almost identical to those of the lipid tails.

The decay of the lipid–lipid correlation intensity is described by the correlation length d_{corr}. In contrast to the mode velocities, d_{corr} increases linearly with area per lipid for all parts of the lipids, with a more pronounced change for the lipid COMs. Furthermore, the time-domain analysis of correlated velocity fluctuations provides an understanding of the exchange of energy relative to thermal fluctuations. The smaller the area per lipid (denser packing), the more pronounced is the dissipation of energy via the collective headgroup motions as indicated by a loss of correlated motions over shorter distances (shorter d_{corr}). However, a weak but significant correlation between the motions of the lipids is still observed for separation distances up to about 20 Å.

More generally, our results point to an overriding effect of hydration on physical biomembrane headgroup properties. In some aspects, this might be akin to solvent effects on protein dynamics[35,36], with one key difference being that the solvation effect does not propagate into the lipid tail region. Furthermore, we speculate that the acoustic modes, as characterised in detail in this work, might play a functional role because they can provide a means to propagate and dissipate external mechanical stress. This might be relevant for the membrane to maintain its structural integrity and, as suggested by Aponte-Santamaria and coworkers[18], potentially also establish an ultrafast signaling mechanism between membrane proteins such as mechanosensitive channels. These notions are supported by recent non-equilibrium MD simulations of lateral stress propagation in a DPPC bilayer, which yielded a similar propagation velocity of 1400 ± 500 m/s[18].

An interesting future direction would be to extend the described methodology and analyses for characterizing collective dynamics in lipid bilayers to other systems, such as more complex multi-component membranes. In this context, future work aiming at a better understanding of biological membranes would require to also include membrane proteins and (water-mediated) coupling to the lipids in terms of the collective dynamics[33,37].

Conflicts of interest

There are no conflicts to declare.

Acknowledgments

This work was funded by the Deutsche Forschungsgemeinschaft (DFG, German Research Foundation) under Germany's Excellence Strategy – EXC-2033 – project number 390677874 and an Emmy-Noether grant to L.V.S. (SCHA 1574/3-1). J.C.S. was supported by the Genomic Science Program, Office of Biological and Environmental Research, US Department of Energy (DOE), under Contract FWP ERKP752. The Steinbuch Centre for Computing (SCC), Karlsruhe/Germany, is acknowledged for providing computational resources.

Notes and references

1 S. J. Singer and G. L. Nicolson, *Science*, 1972, **175**, 720–731.
2 K. Simons and E. Ikonen, *Nature*, 1997, **387**, 569–572.
3 E. Sezgin, I. Levental, S. Mayor and C. Eggeling, *Nat. Rev. Mol. Cell Biol.*, 2017, **18**, 361–374.
4 G. Enkavi, M. Javanainen, W. Kulig, T. Róg and I. Vattulainen, *Chem. Rev.*, 2019, DOI: 10.1021/acs.chemrev.8b00538.
5 R. A. Demel and B. De Kruyff, *Biochim. Biophys. Acta*, 1976, **457**, 109–132.
6 H. Ohvo-Rekilä, B. Ramstedt, P. Leppimäki and J. P. Slotte, *Prog. Lipid Res.*, 2002, **41**, 66–97.
7 D. G. Ackerman and G. W. Feigenson, *Essays Biochem.*, 2015, **57**, 33–42.
8 K. Atkovska, J. Klingler, J. Oberwinkler, S. Keller and J. S. Hub, *ACS Cent. Sci.*, 2018, **4**, 1155–1165.
9 J. H. Ipsen, O. G. Mouritsen and M. Bloom, *Biophys. J.*, 1990, **57**, 405–412.
10 X. Cheng and J. C. Smith, *Chem. Rev.*, 2019, DOI: 10.1021/acs.chemrev.8b00439.
11 T. M. Bayerl, *Curr. Opin. Colloid Interface Sci.*, 2000, **5**, 232–236.
12 E. Falck, T. Róg, M. Karttunen and I. Vattulainen, *J. Am. Chem. Soc.*, 2008, **130**, 44–45.
13 M. Rheinstädter, C. Ollinger, G. Fragneto, F. Demmel and T. Salditt, *Phys. Rev. Lett.*, 2004, **93**, 108107.
14 E. Lindahl and O. Edholm, *Biophys. J.*, 2000, **79**, 426–433.
15 S. H. Chen, C. Y. Liao, H. W. Huang, T. M. Weiss, M. C. Bellisent-Funel and F. Sette, *Phys. Rev. Lett.*, 2001, **86**, 740–743.
16 M. C. Rheinstädter, T. Seydel, W. Häußler and T. Salditt, *J. Vac. Sci. Technol. A*, 2006, **24**, 1191–1196.
17 M. Tarek, D. J. Tobias, S.-H. Chen and M. L. Klein, *Phys. Rev. Lett.*, 2001, **87**, 238101.
18 C. Aponte-Santamaría, J. Brunken and F. Gräter, *J. Am. Chem. Soc.*, 2017, **139**, 13588–13591.
19 J. S. Hub, T. Salditt, M. C. Rheinstädter and B. L. de Groot, *Biophys. J.*, 2007, **93**, 3156–3168.
20 T. H. Haines, *Prog. Lipid Res.*, 2001, **40**, 299–324.
21 S. Paula, A. G. Volkov, A. N. Van Hoek, T. H. Haines and D. W. Deamer, *Biophys. J.*, 1996, **70**, 339–348.

22 J. P. M. Jämbeck and A. P. Lyubartsev, *J. Chem. Theory Comput.*, 2012, **8**, 2938–2948.

23 J. P. M. Jämbeck and A. P. Lyubartsev, *J. Chem. Theory Comput.*, 2013, **9**, 774–784.

24 M. Heyden and D. J. Tobias, *Phys. Rev. Lett.*, 2013, **111**, 218101.

25 M. Heyden, *J. Chem. Phys.*, 2014, **141**, 22D509.

26 J. P. Boon and S. Yip, *Molecular hydrodynamics*, Courier Corporation, 1980.

27 F. Sciortino and S. Sastry, *J. Chem. Phys.*, 1994, **100**, 3881–3893.

28 M. L. Berkowitz and R. Vácha, *Acc. Chem. Res.*, 2012, **45**, 74–82.

29 D. Laage, T. Elsaesser and J. T. Hynes, *Chem. Rev.*, 2017, **117**, 10694–10725.

30 A. Debnath, B. Mukherjee, K. Ayappa, P. K. Maiti and S.-T. Lin, *J. Chem. Phys*, 2010, **133**, 174704.

31 J. Das, E. Flenner and I. Kosztin, *J. Chem. Phys.*, 2013, **139**, 065102.

32 Y. von Hansen, S. Gekle and R. R. Netz, *Phys. Rev. Lett.*, 2013, **111**, 118103.

33 O. Fisette, C. Päslack, R. Barnes, J. M. Isas, R. Langen, M. Heyden, S. Han and L. V. Schäfer, *J. Am. Chem. Soc.*, 2016, **138**, 11526–11535.

34 A. Srivastava and A. Debnath, *J. Chem. Phys.*, 2018, **148**, 094901.

35 L. Hong, X. Cheng, D. C. Glass and J. C. Smith, *Phys. Rev. Lett.*, 2012, **108**, 238102.

36 P. W. Fenimore, H. Frauenfelder, B. H. McMahon and F. G. Parak, *Proc. Natl. Acad. Sci. U.S.A.*, 2002, **99**, 16047–16051.

37 S. Capponi, S. H. White, D. J. Tobias and M. Heyden, *J. Phys. Chem. B*, 2019, **123**, 480–486.

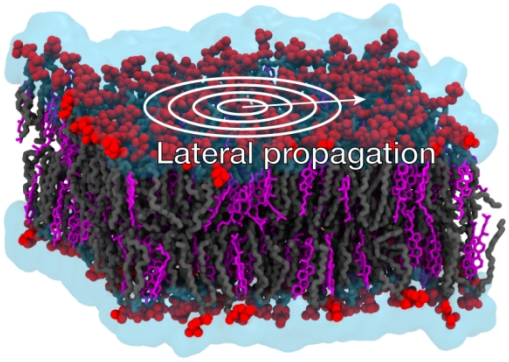
Lateral propagation

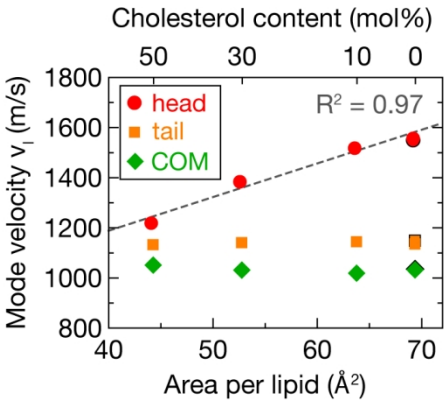
Cholesterol content (mol%)
50
30
10
0
1800
1600
1400
1200
1000
800
Mode velocity v_l (m/s)
head
tail
COM
R^2 = 0.97
40
50
60
70
Area per lipid (Å^2)